Preparation and Assessment of a Polysafranin/Multiwall Carbon Nanotube-Nafion Hybrid Film–Modified Carbon Paste Electrode and Its Performance as an Easy Sensing Probe for H_2O_2 and Cu^{2+}

M. Sayahpour [1] · S. Hashemnia [1] · Z. Mokhtari [2]

Abstract

A polysafranin/multiwall carbon nanotube-Nafion hybrid film was prepared by electropolymerizing safranin on the surface of a MWCNT-Naf/CPE. The modified electrode was evaluated as an electrochemical sensor for hydrogen peroxide (H_2O_2) and Cu^{2+} in the presence of H_2O_2, in 0.1 M Tris buffer (pH 6.0) using cyclic and differential pulse voltammetric methods. The electrode showed a pair of well-defined and quasi-reversible redox peaks with formal potential ($E°$) = 0.290 ± 0.005 V versus Ag/AgCl corresponding to the polysafranin redox couples. The effects of the experimental variables on the electrode behavior regarding polymerization conditions, electrolyte pH, and MWCNT concentration were investigated to obtain optimum experimental conditions. The investigation of differential pulse voltammetric results showed that the polysafranin film at the modified electrode surface acts as an effective catalyst for H_2O_2 r and Cu^{2+} reduction in the presence of H_2O_2. Under optimum conditions, the modified electrode exhibited a linear dynamic range of 4.5–23.0 mM and a sensitivity of 17.4 ± 0.4 µA mM^{-1} cm^{-2} toward H_2O_2 with a detection limit of 0.6 mM ($3S_{bl}$/m). In the presence of 17.0 mM H_2O_2, the electrode showed a linear response range of 1.0–80.0 µM and a sensitivity of 7.6 ± 0.2 µA $µM^{-1}$ cm^{-2}, with a detection limit of 0.1 µM ($3S_{bl}$/m) for Cu^{2+}. In the next step, using differential pulse voltammetry, the response of the electrode to Cu^{2+} was studied in the presence of interfering metal ions that can promote Fenton's reaction. The results showed that Fe^{2+}, Co^{2+}, and Al^{3+} produce interference at more than 5-, 2- and 10-fold ratios ([cation]/[Cu^{2+}]) respectively.

Keywords Electropolymerization; Polysafranin · Hydrogen peroxide · Copper (II) cation

Introduction

In recent years, fabrication and application of electrochemical sensors based on modification of electrode surfaces have increased extensively. The modification of the electrode surface with different materials such as electroactive polymers and nanomaterials leads to an increase in the effective surface area, and enhancing the electrocatalytic activity and sensitivity of the corresponding sensors [1–4]. Among the several types of electrode modifiers, polyazine dyes have received

considerable attention because of their effective role in electron transfer between the electrode surface and analytes. Safranin is an azonium dye which is known as basic red 2, Safranin O, and 3,7-diamino-5-phenylphenazinium chloride. It is an electroactive polyaromatic cation and its electrochemical oxidation can lead to the formation of an electrically conducting polymer film at the electrode surface. This film has good adhesion and can be used as a redox mediator for the detection and quantification of analytes such as hydrogen peroxide (H_2O_2) and transition metals [5, 6]. Furthermore, there is considerable attention to improving electrochemical performance of electrodes by using carbon-based nanomaterials [7–11]. Therefore, the simultaneous use of nanomaterials and conducting polymers synergizes the advantageous features of nanomaterials and conducting polymers which can be applied for modification of electrodes [12–20].

The literature survey shows that, although there are various methods such as volumetric methods [21] and spectrophotometry [22–25] for the determination of hydrogen peroxide

✉ S. Hashemnia
shashemnia@pgu.ac.ir

1   Department of Chemistry, Faculty of Sciences, Persian Gulf University, Bushehr 75169, Iran

2   Department of Chemistry, Yasouj University, Under Hill, Yasouj 75918-74934, Iran

(H₂O₂) and transition metals, voltammetric techniques are good candidates for the development of fast, easy, sensitive, and low-cost methods to investigate hydrogen peroxide and trace amounts of important elements such as copper in aqueous solutions [26–33]. In recent years, increasing attention has been paid to the use of modified electrodes for the detection of the above-mentioned compounds because they have excellent electrical and mechanical properties. Also, they show a high sensitivity, have a low detection limit, and need short analytical time [7–20, 34–37].

In this study, we developed a novel sensor for identification and determination of hydrogen peroxide and copper (II) cation in the presence of hydrogen peroxide by electropolymerization of safranin on the surface of a carbon paste electrode modified with multiwall carbon nanotube-Nafion film (PSF/MWCNT-Naf/CPE) as the working electrode. We tried to evaluate the electrocatalytic response of the electrode toward copper (II) cation based on Fenton-type reactions. Although there are some studies on the electropolymerization of azonium dyes on different electrode surfaces and their use as electrochemical sensors [38–40], to the best of our knowledge, none of the studies has used PSF/MWCNT-Naf/CPE as a modified electrode for sensing hydrogen peroxide and especially trace amounts of copper (II) cation.

Experimental

Materials

All chemicals were of analytical grade and used as received. Hydrogen peroxide (30%) was purchased from Merck. Nafion (5% in ethanol) and safranin were obtained from Aldrich. All experiments were performed at 25.0 °C. Tris buffer (0.1 M, pH 6.0) was used for the preparation of all sample solutions.

Apparatus

A Zahner Zennium potentiostat/galvanostat was used for electrochemical measurements. A three-electrode cell system was used with a PSF/MWCNT-Naf/CPE as the working electrode, an Ag/AgCl electrode as a reference, and a platinum rod as a counter electrode.

Fabrication of the Working Electrode

A homogeneous carbon paste was made by hand mixing of paraffin oil and graphite powder (25:75, w/w %) and was packed into a Teflon tube (ca. 3.0 mm diameter) and smoothed on a weighing paper. Then, 10 μL of Nafion solution (1% in ethanol) containing 1.25 mg/mL multiwall carbon nanotubes which were prepared by sonication for 2 h was cast on the

electrode surface and dried in an oven at 80.0 °C for 3 min. The electrode was immersed in an electrochemical cell containing safranin (5.0 mM) and Tris buffer (0.1 M, pH 6.0). The electropolymerization was performed by cyclic voltammetry in the potential range between - 0.8 and + 1.2 V, for 30 cycles at a scan rate of 50.0 m Vs⁻¹. The electrode was washed with water and dried for further use. The electrolyte solution was purged with the nitrogen gas during the electrochemical measurements, to remove dissolved oxygen.

Results and Discussion

Surface Morphology of the Modified Electrode

Field emission scanning electron microscopy (FESEM) was used to examine the surface morphology of the modified electrode in the different steps of the modification (Fig. 1). Figure 1 a and b show the electrode surface modified with a multiwall carbon nanotube film (MWCNT/CPE) and the surface modified with a multiwall carbon nanotube-Nafion film (MWCNT-Naf/CPE) respectively. As seen, the MWCNT were successfully coated by a thin layer of Nafion. However, after electropolymerization (Fig. 1c), the electrode surface showed a cloudy smooth surface. Therefore, the FESEM images showed a significant difference in the surface morphology, which confirmed the formation of a PSF film on the electrode surface.

Electropolymerization of Safranin

Figure 2a shows the cyclic voltammograms of electropolymerization of safranin on the MWCNT-Naf/CPE in a solution containing 5.0 mM of safranin at a scan rate of 50.0 m Vs⁻¹ in the potential range between - 0.8 and + 1.2 V. As seen in the inset of Fig. 2a, with increasing the number of cyclic scans up to 30 cycles, the redox peak currents gradually increase. This means that the electropolymer film is formed and accumulated on the electrode surface. Further increases in cycles showed a decrease in the redox peak currents, perhaps due to the increase in the film thickness. During the electropolymerization process and, therefore, in the presence of safranin (5.0 mM), the voltammograms showed a multiple peak profile. In this profile, the redox couple with a more negative formal potential corresponds to the reaction of the safranin monomers contained in the polymer structure. The redox couple at the more positive potentials was attributed to the redox reaction of the nitrogen atom of the -NH₂ group of the safranin polymer deposited on the electrode surface. At high anodic potentials, around 1.0 V, an irreversible anodic peak is seen corresponding to the electrochemical formation of the cation radical which is followed by a chemical reaction resulting in polymerization. It is noteworthy that the cyclic
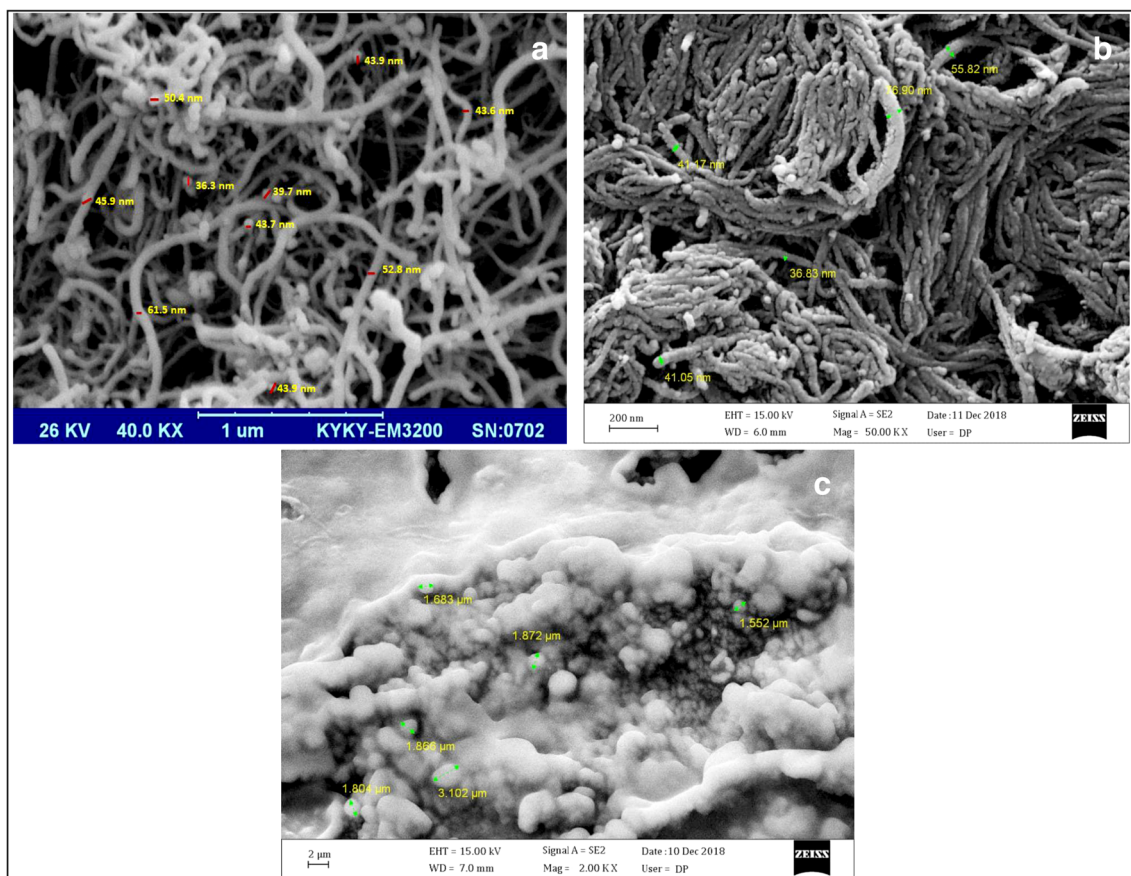
Fig. 1 FESEM images of MWCNT/CPE (**a**), MWCNT-Naf/CPE (**b**), PSF/MWCNT-Naf/CPE (**c**)

voltammograms of safranin molecules at first cycle, before the initiation of polymerization process (dash line), and after the 30th cycle (solid line) are the same, which emphasizes the overlap of the monomer and polymer redox peaks [38, 39]. The safranin molecule is a phenazine compound which exhibits a remarkable delocalization of positive charge over the three nitrogen atoms including both amine groups and the nitrogen ring [40–43]. This charge distribution brings three resonance forms for safranin (cationic) dye (Fig. 2b). It is obvious that the iminium ion resonance forms can participate in redox reactions. A possible mechanism for the redox reaction of safranin monomers is shown in Fig. 2b. As seen, the electrochemical reaction is associated with a two-electron and two-proton transfer processes.

The electrochemical reaction that leads to the safranin electropolymerization can be expressed in terms of the formation of the dication radical of the safranin during the oxidation reaction. The safranin monomer as an aromatic amine has electron donor properties and a high tendency to be oxidized. Monomer oxidation takes place under the applied potential. During this process, the radical cation site is generated in the monomer molecule, thus initiating the polymerization reaction. The structural properties of the polymer, such as the length distribution and the growing branches, are related to

the number of radicals. This oxidative polymerization may be considered as the formation of a covalent bond between monomer molecules with the loss of two protons (Fig. 3). Therefore, safranin electropolymerization is dependent on the pH of the safranin solution [40–46]. Figure 2c shows the cyclic voltammograms of the electropolymerized safranin film on the modified electrode surface, providing different safranin solution pH levels (4.0–9.0). As seen in the inset of Fig. 2c, the highest cathodic and anodic peak currents were obtained at pH 6.0. Therefore, the optimum pH value was selected as 6.0 for later studies.

Cyclic Voltammetry of PSF/MWCNT-Naf/CPE

The cyclic voltammogram of the modified electrode (PSF/MWCNT-Naf/CPE) was recorded in 0.1 M potassium chloride and 0.1 M Tris buffer at pH 6.0 with a scan rate of 100.0 m Vs^{-1} in the potential range of − 0.8 to 1.2 V (Fig. 4a). As seen in the figure, PSF/MWCNT-Naf/CPE shows a pair of well-defined, quasi-reversible redox peaks with a peak to peak separation ($\Delta E_p = E_{pa}$- E_{pc}) of 431.0 mV and the value of I_{pa}/I_{pc} equal to 0.6 which is attributed to the reduction and oxidation of the polysafranin on the electrode surface (PFS$_{ox}$/PFS$_{red}$ redox couples). The formal
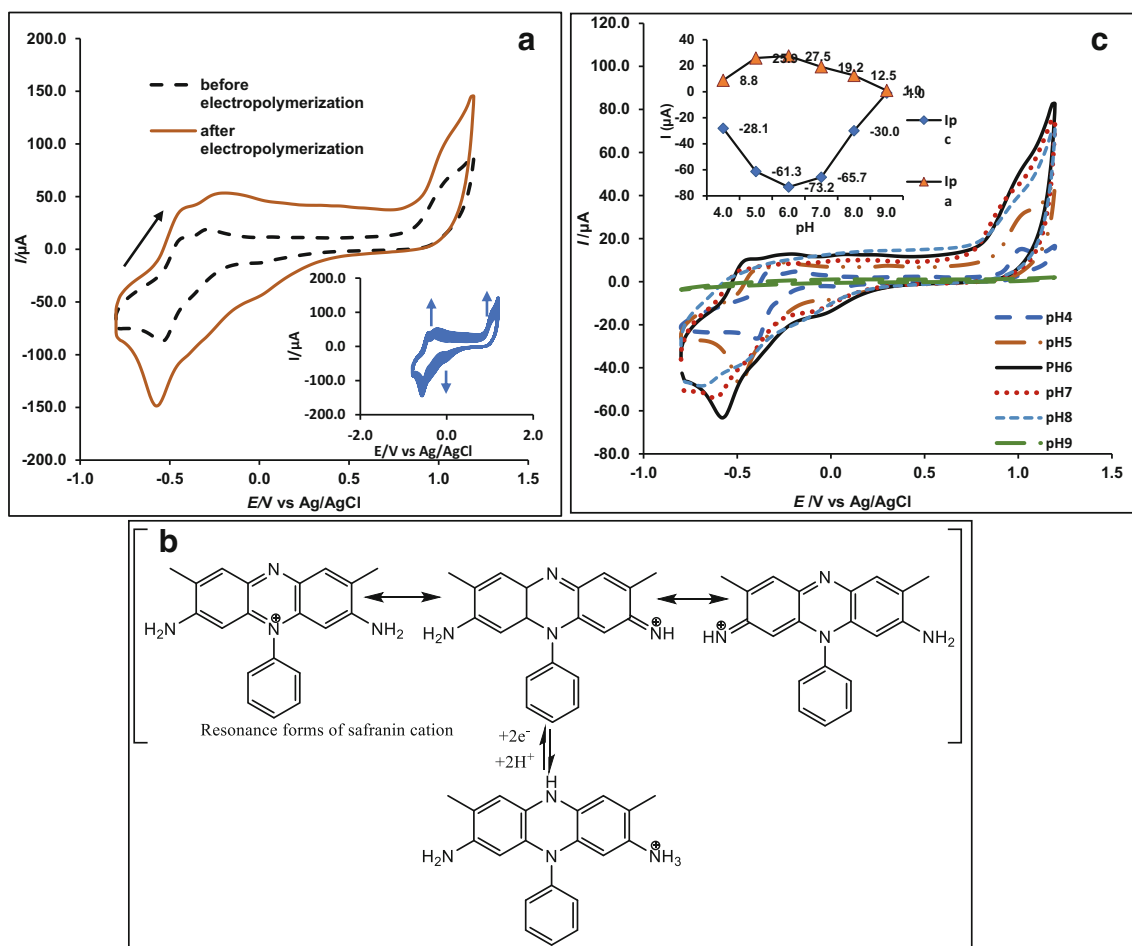
Fig. 2 **a** The cyclic voltammograms of the first cycle and the 30th cycle of the safranin electropolymerization on the MWCNT-Naf/CPE. The inset indicates the consecutive cyclic voltammograms recorded during the electropolymerization process. Conditions: 5.0 mM safranin, 0.1 M potassium chloride, and 0.1 M Tris buffer at pH 6.0 in the potential range of -0.8 to 1.2 V and scan rate 50 m Vs^{-1}. **b** Resonance forms of safranin cation and the possible mechanism of the safranin redox reaction. **c** The cyclic voltammograms of the formed PSF during the electropolymerization process at the MWCNT-Naf/CPE surface at different pHs (4.0–9.0) with a scan rate of 50.0 mV s^{-1} The inset of b indicates the plot of $I/\mu A$ vs. pH in electrolyte solution containing 5.0 mM safranin, 0.1 M potassium chloride, and 0.1 M Tris buffer

potential ($E°$) of the polysafranin on the electrode surface was calculated from the equation $E° = (E_{pa} + E_{pc})/2$ and the result was 290.0 ± 3.0 mV versus Ag/AgCl. No peak was observed for the CPE, MWCNT/CPE, and MWCNT-Naf/CPE in the same potential range.

To obtain the best electrochemical performance of PSF/MWCNT-Naf/CPE, the parameters including pH, scan rate, and MWCNT amount were optimized. The highest peak currents were obtained when the CPE was modified with 1.25 mg/mL MWCNT. The electrochemical response of the PSF/MWCNT-Naf/CPE is, generally, pH-dependent. Thus, the electrochemical performance of the modified electrode was investigated in different pHs of the buffer solution by the cyclic voltammetry method. As seen in Fig. 4 B1 and B3, the formal potential of the PFS shifts negatively with the increase of pH in the range of 3.0 to 8.0. The plot of formal potential versus pH shows a straight line with a slope of $-$

60.0 mV/pH, which indicates that the electrode reaction was accompanied by the two-electron/two-proton process [43, 45–47]. The best response current was achieved at a pH of about 6.0 (Fig. 4 B2). Therefore, to obtain maximum sensitivity, pH 6.0 was chosen in the subsequent experiments. The observed redox behavior can be assigned to the electropolymerized safranin molecules at the MWCNT-Naf surface. Nafion is a polymer consisting of a hydrophilic ionic component and a hydrophobic perfluorocarbon backbone, so the side chain fluorocarbon of the Nafion polymer reacts with the MWCNT surfaces and the negatively charged sulfonated groups impose to the aqueous solution. Hence, Nafion can stimulate the mobility of the cationic safranin molecules toward the modified electrode and can stabilize the resultant cationic polymer on the electrode surface (Fig. 4 C1). In these circumstances, a two-electron and two-proton process can occur on the modified electrode surface and the oxidation of the

Fig. 3 The possible mechanism for the formation of the electropolymerized safranin film by the dication radicals formed through the oxidation reaction of safranin

Safranin dicaion radical

Safranin cation

Safranin nitrenium cation

Safranin dimer
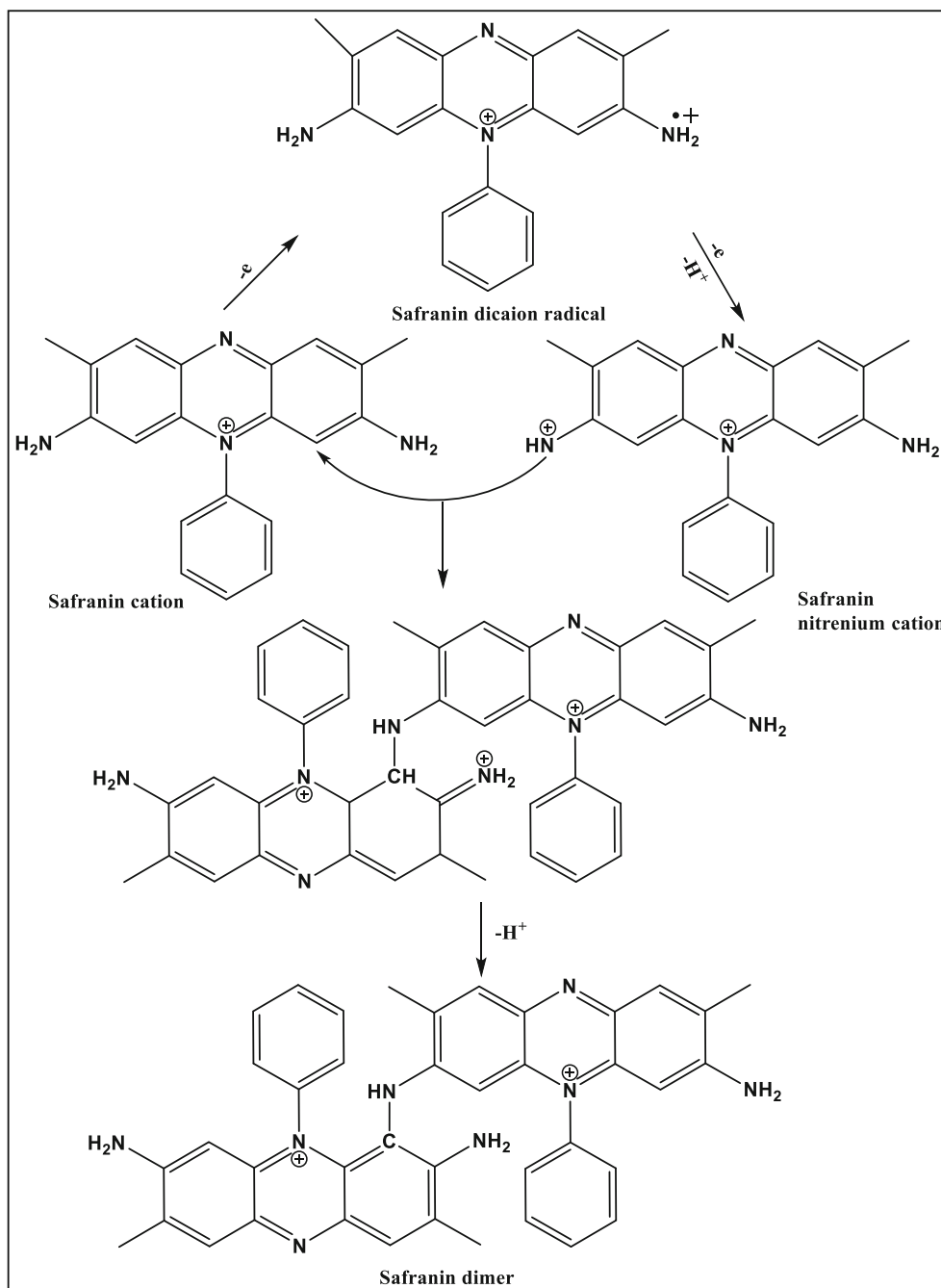
cationic polymer can lead to the formation of a dihydrophenazine-like structure (Fig. 4 C2) [40, 41, 45].

Electrocatalytic Reduction of H₂O₂

Figure 5 a and b exhibit the cyclic voltammograms (CVs) and differential pulse voltammograms (DPVs) of PSF/MWCNT-Naf/CPE in Tris buffer at pH 6.0 in the presence of various concentrations of H_2O_2, respectively. As seen in Fig. 5a, there is an increase in the reduction peak current with increasing the H_2O_2 concentration. The increase in the reduction peak current is accompanied by the decrease of the corresponding oxidation peak current, which is characteristic of an electrochemically catalytic reaction. Therefore, the PSF on the electrode surface can act as a potent catalyst for the reduction of H_2O_2 (5D). DVPs show along with increasing the concentration of H_2O_2 the reduction peak current of PSF (I_{pc}) at − 370.0 mV decreases, and two new reduction peaks at potentials 90.0 mV (I_{pc1}) and − 650.0 mV (I_{pc2}) begin to appear and increase gradually. It seems in the presence of H_2O_2 the product of PSF oxidation (Fig. 4 C2), being oxidized further [40],
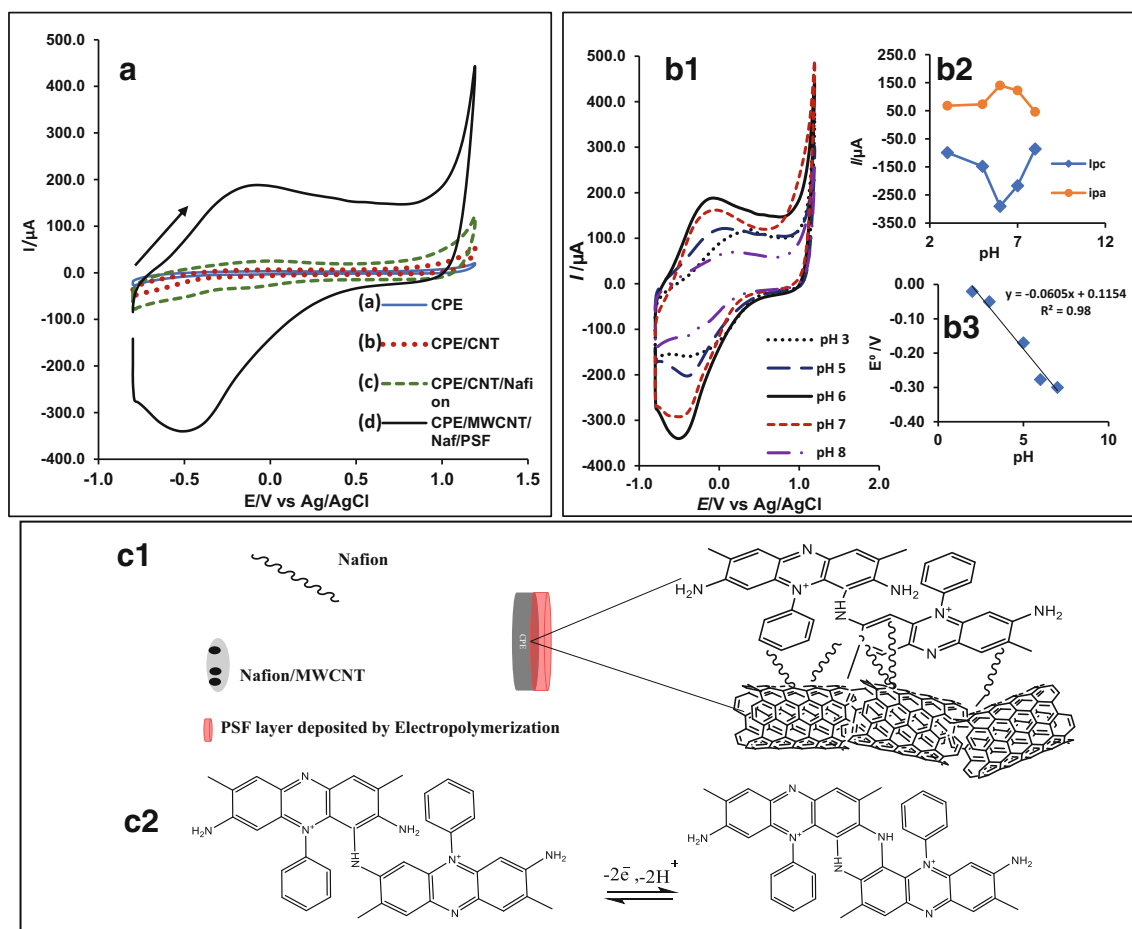
Fig. 4 **a** The cyclic voltammograms of the (a) CPE, (b) MWCNT/CPE, (c) MWCNT-Naf/CPE, and (d) PSF/MWCNT-Naf/CPE in electrolyte solution containing 0.1 M potassium chloride, and 0.1 M Tris buffer, pH 6.0 with a scan rate of 100.0 m Vs^{-1}. **b** Dependence of peak potential and peak current of PSF on pH of the electrolyte solution; (b1) cyclic voltammograms of the modified electrode (PSF/MWCNT-Naf/CPE) obtained in Tris buffer solutions at various pHs (3.0–8.0). (b2) The plot of the maximum reduction current, I/μA, versus pH. (b3) The plot of the formal potential ($E°$) versus pH (3.0–8.0) for the modified electrode. Condition: 0.1 M potassium chloride, and 0.1 M Tris buffer in the potential range of − 0.8 to 1.2 V. **c** (c1) a proposed schematic for modification of the MWCNT-Naf/CPE with electrodeposition of the PSF to form the PSF/ MWCNT-Naf/CPE, (c2) a possible electron transfer process on the modified electrode surface (PSF/MWCNT-Naf/CPE)

and the resulting products can be reduced at the electrode surface at the above- mentioned potentials.

The effect of varying amounts of H$_2$O$_2$ on I_{pc1} is remarkably more than that of I_{pc2} (Fig. 5b). The I_{pc1} is linearly proportional to the concentration of H_2O_2 in the range of 4.5 to 23.0 mM with the regression equation I_{pc1}/μA = 1.2(± 0.3 × 10–1) × C + 15.3(± 0.4) (C in mM, R^2 = 0.99) (Fig. 5c). The modified electrode shows a sensitivity of 17.5 ± 0.4 μA mM^{-1} cm^{-2} for H$_2$O$_2$. The limit of detection, C_m, was estimated by using the equation $C_m = 3S_{bl}/m$, where $S_{bl} = 2.7 \times 10$–1 μA is the standard deviation of the cathodic peak current in the absence of H$_2$O$_2$ (10 replicates) and m is the slope of the calibration curve. Analyzing these data, we estimate that the detection limit of H$_2$O$_2$ is 0.6 mM. A comparison of the electroanalytical performance of PSF/ MWCNT-Naf/CPE with some other previously reported

modified electrodes indicated that the modified electrode has acceptable electrocatalytic activity and rapid response time toward hydrogen peroxide oxidation and reduction [48–50]. It is noteworthy that H$_2$O$_2$ showed no voltammetric peaks in the abovementioned potential window at the surface of the bare CPE (Fig. 5a). From the analytical point of view, there are many reports that present a better result than our result [3, 4, 7–16]. However, the stability and the fast response of the electrode make it suitable for investigating the mechanistic aspect of this work and also the determination of Cu^{2+} in the presence of hydrogen peroxide (next section).

Electrocatalytic Reduction of Cu^{2+}

Figure 6a exhibits the cyclic voltammograms of the modified electrode in 0.1 M Tris buffer at pH 6.0 in the presence of (a)
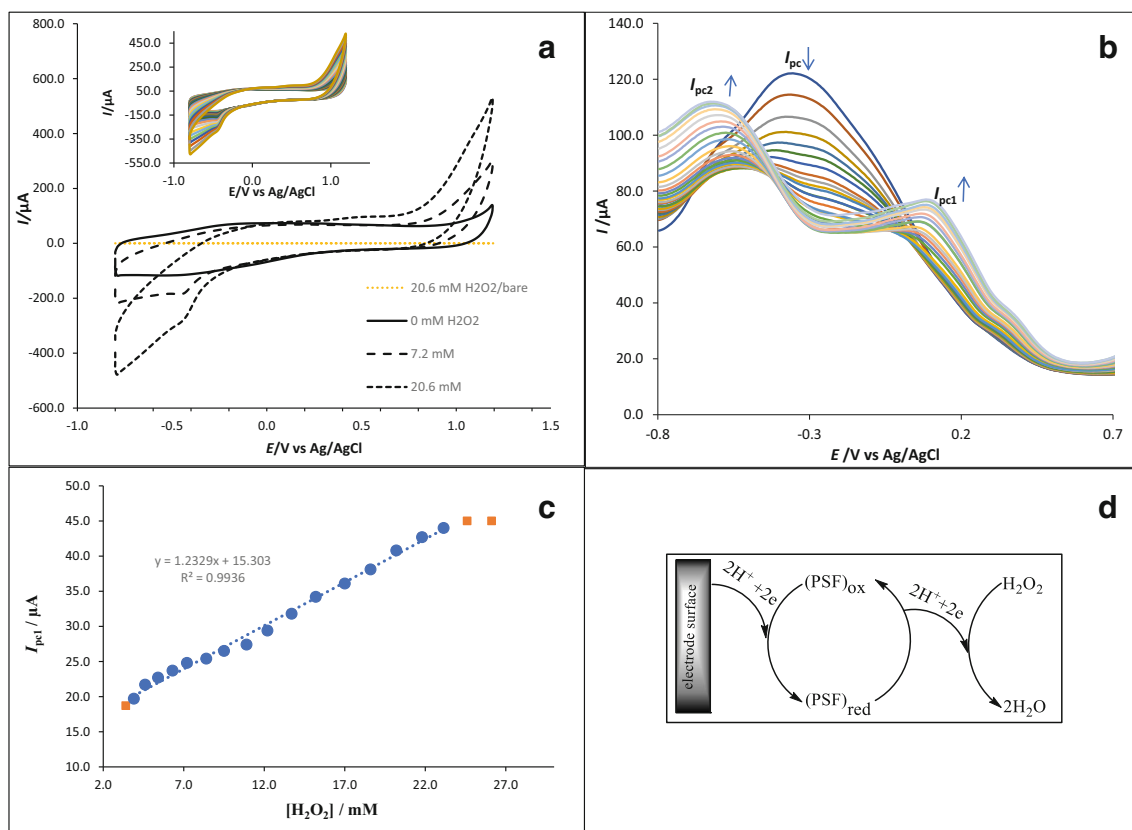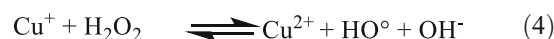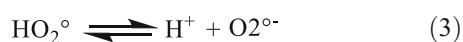
Fig. 5 **a** and **b** show the cyclic voltammograms and cathodic differential pulse voltammograms of the modified electrode in the presence of various amounts of H_2O_2, respectively. **c** Calibration curve of the modified carbon paste electrode obtained from differential pulse voltammetry data. **d** A suggested mechanism for catalytic reduction of H_2O_2 on the surface of the modified electrode

Cu^{2+} (0.0 μM)/H_2O_2 (0.0 mM), (b) Cu^{2+} (0.0 μM)/H_2O_2 (17.0 mM), (c) Cu^{2+} (20.8 μM)/H_2O_2 (17.0 mM), and (d) Cu^{2+} (48.7 μM)/H_2O_2 (17.0 mM). As the figure shows, adding Cu^{2+} to the buffer solution containing H_2O_2 (17.0 mM) leads to a more significant increase in the reduction peak current. The increase in the reduction peak current is accompanied by a decrease in the corresponding oxidation peak current. This result shows that in the presence of Cu^{2+}, the PSF film on the electrode surface can act as a potent catalyst for the reduction of OH^0 which is produced during the Fenton-like (cupro-Fenton) reaction. According to the literature, Cu^{2+} can convert to Cu^+ and produce large amounts of $OH^°$ in the presence of excess H_2O_2 (Eqs. 1–4) [51, 52] (Fig. 6d). Regardless of the mechanism by which H_2O_2 may react with Cu^{2+} to form Cu^+, it is possible that the obtained $O_2^{°-}$ reacts with Cu^{2+} to produce Cu^+ ($Cu^{2+} + O_2^{°-} \rightarrow Cu^+ + O_2$), which means that even more Cu (I) can be formed.

$$H_2O_2 \rightleftharpoons H^+ + HOO^- \qquad (1)$$

$$Cu^{2+} + HOO^- \rightleftharpoons Cu^+ + HO_2^° \qquad (2)$$

$$HO_2^° \rightleftharpoons H^+ + O2^{°-} \qquad (3)$$

$$Cu^+ + H_2O_2 \rightleftharpoons Cu^{2+} + HO^° + OH^- \qquad (4)$$

In these circumstances, PSF_{ox} can accept two electrons from the electrode and two protons from the solution to change into PSF_{red}. In the second step, PSF_{red} is changed into PSF_{ox} by hydroxyl radicals produced from cupro-Fenton's reaction. Therefore, the increasing Cu^{2+} ion concentration causes an increase in the amount of PSF_{ox} species and, finally, enhances the reduction peak current. It is noteworthy that the hydrogen peroxide concentrations above 17.00 mM did not affect the electrode response toward Cu^{2+}. Figure 6b shows the differential pulse voltammetric investigation of Cu^{2+} on the surface of the modified electrode in the presence of H_2O_2 with more details. Here too, the product of the reaction of PSF with H_2O_2 shows two reduction peaks (Fig. 4 C2), and the currents of both reduction peaks, I_{pc1} and I_{pc2}, are increased by increasing the Cu^{2+} concentration. I_{pc1} is more strongly affected by varying Cu^{2+} concentrations than I_{pc2} and the intensity of I_{pc1} is linearly proportional to the Cu^{2+} concentration in the range of 1.0 to 80.0 μM with the regression equation I_{pc1}/μA = 0.5 ($\pm 0.1 \times 10-1$) × C + 118.0 (± 0.4) (C in mM, R^2 = 0.99) (Fig. 6c). The modified electrode exhibits a sensitivity of 7.6 ± 0.2 μA μM^{-1} cm^{-2} for Cu^{2+}. The limit of detection, C_m, was estimated by using the equation $C_m = 3S_{bl}/m$, where $S_{bl} =$
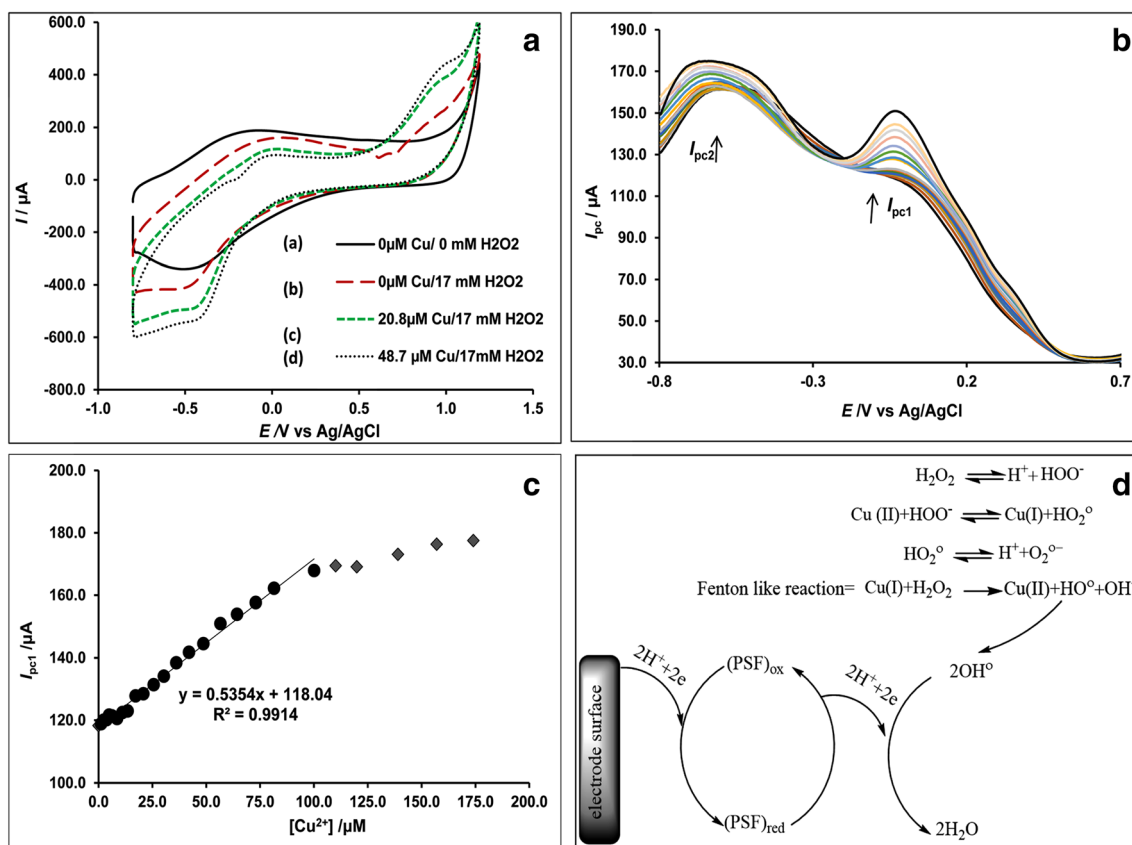
Fig. 6 a The cyclic voltammograms of the modified electrode in the presence of various amounts of Cu^{2+}. **b** The cathodic differential pulse voltammograms of the modified electrode in the presence of various amounts of Cu^{2+}. **c** Calibration curve of the modified carbon paste electrode obtained from differential pulse voltammetric data. **d** Suggested mechanism for catalytic reduction of Cu^{2+} on the surface of the modified electrode

0.1×10^{-1} μA is the standard deviation of the cathodic peak current in the absence of Cu^{2+} (10 replicates) and m is the slope of the calibration curve. With the analysis of these data, we estimated that the detection limit of Cu^{2+} was 0.1 μM. It is noteworthy that Cu^{2+} showed no voltammetric peaks for the Cu^{2+} ions in the above mentioned potential window at the surface of the bare CPE. Table 1 exhibits the comparison of detection limit and dynamic linear range values of the modified electrode for Cu^{2+} and some literature values [52–56]. As seen in the figure, the method has a lower limit of linear response toward Cu^{2+} than some other reports in the literature. To evaluate the application of the modified electrode, some

Table 1 Comparison of the electrochemical performance of PSF/MWCNT-Naf/CPE with other reported electrodes toward Cu^{2+}

Method	Modified electrode	Linear range (μM)	Detection limit (1 μM)	reference
DVP[a]	MGCE[d]	10.0-2000.0	10.0	54
DPASV[b]	L-cysteine MGE[e]	2.0–20.0	1.3×10^{-1}	55
LASV[c]	MCPE[f]	0.8–10.0	0.2	56
DPASV	MCPE-CNT[g]	0.06–3.1	1.7×10^{-2}	57
DPV	PSF/MWCNT-Naf/CPE	1.0–80.0	0.1	This work

[a] Differential pulse voltammetry

[b] Differential pulse cathodic stripping voltammetry

[c)] Linear anodic stripping voltammetry

[d] Modified glassy carbon electrode with *N, N′*-bis(acetylacetone)ethylenediimine

[e] L-cysteine modified gold electrode

[f] Modified carbon paste electrode with organo-functionalized SBA-15 nanostructured silica

[g] Modified carbon paste electrode with dicyclohexyl-18-crown-6 and multi-walled carbon nanotubes

Table 2 Determination of some Cu^{2+} standard solutions by the proposed method. Copper (Cu^{2+}) concentrations were confirmed by atomic absorption spectroscopy

$[Cu^{2+}](\mu M)$	Measured $[Cu^{2+}](\mu M)$	Recovery%
20.8	22.0	105.7
42.0	40.0	95.2
75.0	74.7	99.6

Cu^{2+} samples were determined by the standard addition method. The Cu^{2+} concentrations were confirmed by atomic absorption spectroscopy. The results presented in Table 2 seem to be satisfactory.

Interferences Study

The response of the electrode to Cu^{2+} (36 μM) in the presence of metal ions that can promote Fenton reaction (such as Fe^{2+}, Co^{2+}, and Al^{3+}) was examined by the differential pulse voltammetry technique. The maximum amount of the cations that can cause an error of up to 5% on the peak current of Cu^{2+} (I_{pc1}) was considered the maximum tolerance level. As seen in Table 3, Fe^{2+}, Co^{2+}, and Al^{3+} have interferences at the ratios ($[cation]/[Cu^{2+}]$) more than 5-, 2-, and 10-fold respectively.

Stability, Reproducibility, and Repeatability

The stability of the modified electrode was investigated by cyclic voltammetry in the potential range of −0.8 to 1.2 V. Results showed that after 20 cycles, the cathodic and anodic peak potentials remained nearly unchanged while the anodic and cathodic peak currents reduced by 1.7% and 0.7% respectively. Furthermore, results showed the cathodic peak current decreased to about 93% of its first value after 2 days.

The reproducibility of the electrode was estimated by preparing five electrodes under the same conditions. The relative standard deviation (% R.S.D.) was 5.3% for an average of 322.6 μA for the cathodic peak current.

The repeatability of the modified electrode was examined by measuring the cathodic current toward 17.0 mM H_2O_2 and 48.7 μM Cu^{2+} in the presence of 17.0 mM of hydrogen

Table 3 Effect of interfering metal ions on the electrode response to Cu^{2+}. The recovery was calculated by comparing the electrode response to Cu^{2+} (36 μM) in the presence and absence of the interfering metal ions

Foreign ion	$[Cation]/[Cu^{2}]$	Recovery%
Fe^{2+}	5.0	103.9
Co^{2+}	2.0	104.5
Al^{3+}	10.0	95.4

peroxide. The relative standard deviations for three successive measurements were 4.8% and 3.2% respectively.

Conclusions

In this work, the electropolymerization technique was applied to construct a hybrid conductive film of PSF/MWCNT-Naf at CPE. The FESEM images revealed the formation of PSF. Results demonstrated that the PSF/MWCNT-Naf/CPE can act as an electrochemical sensor for the detection of H_2O_2 and trace amounts of copper (II) cation in the presence of H_2O_2. The proposed electrochemical sensor exhibited fast response, low cost, high sensitivity, stability, and simplicity in fabrication and manipulation. So, the development of this new method for the analysis of H_2O_2 and trace amounts of copper (II) cation is beneficial, especially with regard to some properties of the method such as cost effectiveness, fast response, and safety.

References

1. V.S. Manikandan, B. Sidhureddy, A. Thiruppathi, A. Chen, Sensitive electrochemical detection of caffeic acid in wine based on fluorine-doped graphene oxide. Sensors **19**(7), 1604 (2019)
2. R. Zhang, W. Chen Biosens, Recent advances in graphene-based nanomaterials for fabricating electrochemical hydrogen peroxide sensors. Bioelectron. **89**(Pt 1), 249–268 (2017)
3. A. Manivel, S. Anandan, J. Solid State Electrochem. **15**, 153 (2010)
4. H.W. Siao, S.M. Chen, K.C. Lin, J. Solid State Electrochem. **15**, 1121 (2010)
5. R. Herrero, R. Guidelli, Adsorption and reduction kinetics of safranine T in self-assembled phospholipid monolayers deposited on mercury. J. Electroanal. Chem. **425**(1-2), 87–95 (1997)
6. R. Pauliukaite, M.E. Ghica, M.M. Barsan, C.M.A. Brett, Phenazines and polyphenazines in electrochemical sensors and biosensors. Anal. Lett. **43**(10-11), 1588–1608 (2010)
7. Y. Li, Y. Li, Y. Yang, A new amperometric H2O2 biosensor based on nanocomposite films of chitosan–MWNTs, hemoglobin, and silver nanoparticles. J. Solid State Electrochem. **16**(3), 1133–1140 (2012)
8. A. Afraz, A.A. Rafati, A. Hajian, Analytical sensing of hydrogen peroxide on Ag nanoparticles–multiwalled carbon nanotube-modified glassy carbon electrode. J. Solid State Electrochem. **17**(7), 2017–2025 (2013)
9. J.V. Da Silva, D.M. Pimentel, D.E.P. Souto, R. de Cassia Silva Luz, F.S. Damos, J. Solid State Electrochem. **17**, 2795 (2013)
10. S. Nalini, S. Nandini, S. Shanmugam, S.E. Neelagund, J.S. Melo, G.S. Suresh, J. Solid State Electrochem. **18**, 685 (2013)
11. M.S. Randjelović, M.Z. Momčilović, D. Enke, V. Mirčeski, Electrochemistry of hydrogen peroxide reduction reaction on carbon paste electrodes modified by Ag- and Pt-supported carbon microspheres. J. Solid State Electrochem. **23**(4), 1257–1267 (2019)
12. X. Liu, L. Luo, Y. Ding, Y. Xu, F. Li, J. Solid State Electrochem. **15**, 447 (2010)

13. J. Wang, L. Cui, H. Yin, J. Dong, S. Ai, J. Solid State Electrochem. **16**, 1545 (2011)

14. L. Wang, H. Zhu, H. Hou, Z. Zhang, X. Xio, Y. Song, J. Solid State Electrochem. **16**, 1693 (2011)

15. R. Wu, X. Chen, J. Hu, J. Solid State Electrochem. **16**, 1975 (2011)

16. Y. Wang, H. Zhang, D. Yao, J. Pu, Y. Zhang, X. Gao, Y. Sun, J. Solid State Electrochem. **17**, 881 (2012)

17. P. Prabhu, R.S. Babu, S.S. Narayanan, J. Solid State Electrochem. **18**, 883 (2013)

18. W.L. Hao, H.X. Li, C.Y. Shen, S.L. Liu, J. Solid State Electrochem. **18**, 1041 (2013)

19. B.P. Crulhas, N.P. Ramos, G.R. Castro, V.A. Pedrosa, Detection of hydrogen peroxide releasing from prostate cancer cell using a biosensor. J. Solid State Electrochem. **20**(9), 2427–2433 (2016)

20. K.G. Nikolaev, V. Maybeck, E. Neumann, Y.E. Ermolenko, A. Offenhausser, Y.G. Mourzina, J. Solid State Electrochem. **22**, 1023 (2017)

21. M.I. Prodromidis, C.D. Stalikas, P.T. Veltsistas, M.I. Karayannis, Spectrophotometric kinetic determination of copper(II) trace amounts based on its catalytic effect on the reaction of the reduced 2,6-dichlorophenolindophenol and hydrogen peroxide. Talanta **41**(10), 1645–1649 (1994)

22. Y.Y. Petrova, M.K. Beklemishev, N.A. Bazhanova, A.A. Druzhinin, I.F. Dolmanova, Determination of copper by its catalytic effect on the oxidation of hydroquinone by hydrogen peroxide on supports. J. Anal. Chem. **55**(3), 284–290 (2000)

23. A. Yeşilkaya, A. Yeĝin, G. Yücel, Y. Alicigüzel, T.A. Aksu, Continuous monitoring of hydroperoxide-induced peroxidation in human erythrocytes by low-level chemiluminescence. Int. J. Clin. Lab Res. **26**(1), 60–68 (1996)

24. A.N. Baga, G.R.A. Johnson, N.B.R.A. Nazhat, Saadalla-Nazhat, Anal. Chim. Acta **204**, 349–353 (1988)

25. K. Helrach, Official Methods of Analysis, 15th edn. (Arlington, AOAC, 1990), Sec. 965.33

26. D. Jin, K. Sakthivel, S. Gandhi, B.T. Huy, Y.I. Lee, An improved non-enzymatic hydrogen peroxide sensor based on europium functionalized inorganic hybrid material—evaluation of optical and electrochemical properties. Sensor Actuat. B-Chem. **237**, 81–89 (2016)

27. Y. Jiang, J.V. Hunt, S.P. Wolff, Ferrous ion oxidation in the presence of xylenol orange for detection of lipid hydroperoxide in low density lipoprotein. Anal. Biochem. **202**(2), 384–389 (1992)

28. K. Ma, F.R. van de Voort, A.A. Ismail, H. Zhuo, B. Cheng, Monitoring peroxide value in fatliquor manufacture by Fourier transform infrared spectroscopy. J. Am. Oil Chem. Soc. **77**(6), 681–685 (2000)

29. H. Ruttinger, A. Radschuweit, Determination of peroxides by capillary zone electrophoresis with amperometric detection. J. Chromatogr. A **868**(1), 127–134 (2000)

30. C.W. Zhang, Oloman, J. Appl. Electrochem. **35**(*10*), 945–*953* (2005)

31. P. Westbroek, J. Hakuzimana, E. Gasana, P. Lombaert, P. Kiekens, Voltammetric detection of hydrogen peroxide in teeth whitening gels. Sensors Actuators B Chem. **124**(2), 317–322 (2007)

32. I. Švancara, K. Vytřas, J. Barek, J. Zima, Carbon Paste Electrodes in Modern Electroanalysis. Crit. Rev. Anal. Chem. **31**(4), 311–345 (2001)

33. B. Uslu, S.A. Ozkan, Electroanalytical application of carbon based electrodes to the pharmaceuticals. Anal. Lett. **40**(5), 817–853 (2007)

34. L. Zou, Y. Li, W. Zhao, S. Zhang, B. Ye, J. Solid State Electrochem. **16**, 505 (2011)

35. Y.Q. Tian, H.Q. Luo, N.B. Li, J. Solid State Electrochem. **16**, 529 (2011)

36. R. Ansari, A.F. Delavar, A. Aliakbar, A. Mohammad-Khan, J. Solid State Electrochem. **16**, 869 (2011)

37. H. Shen, J.E. Mark, C.J. Seliskar, H.B. Mark Jr., W.R. Heineman, Stripping voltammetry of copper and lead using gold electrodes modified with self-assembled monolayers. J. Solid State Electrochem. **1**(3), 241–247 (1997)

38. R. Pauliukaite, M.E. Ghica, M. Barsan, C.M.A. Brett, Characterisation of poly(neutral red) modified carbon film electrodes; application as a redox mediator for biosensors. J. Solid State Electrochem. **11**(7), 899–908 (2007)

39. G. Inzelt, E. Csahók, Electrochemical Quartz Crystal Microbalance Studies of the Formation and Redox Behavior of Poly(Neutral Red) Electrodes. Electroanalysis **11**(10-11), 744–748 (1999)

40. G. Cirić-Marjanović, N.V. Blinova, M. Trchová, J. Stejskal, J. Phys. Chem. B **111**, 2188 (2007)

41. R. Pauliukaite, A. Selskiene, A. Malinauskas, C.M.A. Brett, Electrosynthesis and characterisation of poly(safranine T) electroactive polymer films. Thin Solid Films **517**(18), 5435–5441 (2009)

42. A. Taher, F. Majidi, A. Mohadesi, Electrochemical and electrocatalytic behaviors of Safranin O/Nafion film deposited on the glassy carbon electrode. Russ. J. Electrochem. **45**(10), 1156–1161 (2009)

43. M.M. Barsan, M.E. Ghica, C.M.A. Brett, Electrochemical sensors and biosensors based on redox polymer/carbon nanotube modified electrodes: A review. Anal. Chim. Acta **881**, 1–23 (2015)

44. A.A. Karyakin, E.E. Karyakina, H.L. Schmidt, Electropolymerized azines: a new group of electroactive polymers. Electroanalysis **11**(3), 149–155 (1999)

45. A.A. Karyakin, E.E. Karyakina, W. Schumann, H.L. Schmidt, Electropolymerized azines: Part II. In a search of the best electrocatalyst of NADH oxidation. Electroanalysis **11**(8), 553–557 (1999)

46. W.J. Albery, A.R. Mount, J. Chem. Soc. Faraday Trans. **185**, 1189 (1989)

47. S. Shahrokhian, M. Ghalkhani, Simultaneous voltammetric detection of ascorbic acid and uric acid at a carbon-paste modified electrode incorporating thionine–nafion ion-pair as an electron mediator. Electrochim. Acta **51**(13), 2599–2606 (2006)

48. J.S. Easow, T. Selvaraju, Unzipped catalytic activity of copper in realizing bimetallic Ag@Cu nanowires as a better amperometric H2O2 sensor. Electrochim. Acta **112**, 648–654 (2013)

49. J. Zhou, Y. Zhao, J. Bao, D. Huo, H. Fa, X. Shen, C. Hou, One-step electrodeposition of Au-Pt bimetallic nanoparticles on MoS 2 nanoflowers for hydrogen peroxide enzyme-free electrochemical sensor. Electrochim. Acta **250**, 152–158 (2017)

50. K. Kim, K. Lee, S. So, S. Cho, M. Lee, K. You, J. Moon, T. Song, ECS J Solid State Sci. Technol. **7**, 91 (2018)

51. A.N. Pham, G. Xing, C.J. Miller, T.D. Waite, Fenton-like copper redox chemistry revisited: hydrogen peroxide and superoxide mediation of copper-catalyzed oxidant production. J. Catal. **301**, 54–64 (2013)

52. B. Feier, I. Bǎjan, I. Fizeşan, D. Floner, C. Cristea, F. Geneste, R. Sǎndulescu, Int. J. Electrochem. Sci. **10**, 121 (2015)

53. X. Dai, R.G. Compton, Determination of copper in the presence of various amounts of arsenic with L-cysteine modified gold electrodes. Electroanalysis **17**(20), 1835–1840 (2005)

54. I. Cesarino, G. Marino, J. do Rosario Matos, E.T.G. Cavalheiro, Talanta **75**, 15 (2008)

55. M. Nasiri-Majd, M.A. Taher, H. Fazelirad, Preparation and application of a simple electrochemical sensor for the determination of copper in some real and standard samples. Ionics **22**(2), 289–296 (2016)

56. H.B. Noh, K.S. Lee, P. Chandra, M.S. Won, Y.B. Shim, Electrochim. Acta **61** (2012)